UCRL 3093
Cy. 2

UNIVERSITY OF CALIFORNIA

Ernest O. Lawrence Radiation Laboratory

TWO-WEEK LOAN COPY

This is a Library Circulating Copy which may be borrowed for two weeks. For a personal retention copy, call Tech. Info. Division, Ext. 5545

BERKELEY, CALIFORNIA

DISCLAIMER

This document was prepared as an account of work sponsored by the United States Government. While this document is believed to contain correct information, neither the United States Government nor any agency thereof, nor the Regents of the University of California, nor any of their employees, makes any warranty, express or implied, or assumes any legal responsibility for the accuracy, completeness, or usefulness of any information, apparatus, product, or process disclosed, or represents that its use would not infringe privately owned rights. Reference herein to any specific commercial product, process, or service by its trade name, trademark, manufacturer, or otherwise, does not necessarily constitute or imply its endorsement, recommendation, or favoring by the United States Government or any agency thereof, or the Regents of the University of California. The views and opinions of authors expressed herein do not necessarily state or reflect those of the United States Government or any agency thereof or the Regents of the University of California.

UCRL-3093

UNIVERSITY OF CALIFORNIA

Radiation Laboratory
Berkeley, California

Contract No. W-7405-eng-48

SYSTEMATICS OF EXCITATION FUNCTIONS WITH APPLICATION TO LEAD

Walter John, Jr.

(Thesis)

August 4, 1955

Printed for the U. S. Atomic Energy Commission

Contents

Abstract 3
I. General Introduction 4
II. Alpha-Induced Reactions on Lead
1. Introduction 8
2. Study of the reactions on lead 8
III. Experimental Methods
1. Preparation of targets 12
2. Bombardment 14
3. Counting 20
IV. Results
1. Measured cross sections 23
2. Errors in the cross sections 23
3. Yields of Po^{206}, Po^{207}, and Po^{209} 31
V. Discussion
1. Test of the predictions of Bohr's compound nucleus theory 33
2. General features of the excitation functions in the region of lead 36
3. Total cross sections 40
Acknowledgments 41
References 42

SYSTEMATICS OF EXCITATION FUNCTIONS WITH APPLICATION TO LEAD

Walter John, Jr.

Radiation Laboratory
University of California
Berkeley, California

August 4, 1955

ABSTRACT

The excitation functions for alpha-induced reactions on lead have been measured. A procedure has been developed for preparing enriched lead isotope targets by evaporation. Stacked foils were bombarded by the alpha-beam of the 60-inch cyclotron. The induced polonium alpha activities were separated by alpha pulse-height analysis.

The measured excitation functions for $Pb^{206} + \alpha$ are compared to the excitation functions for Bi + p. Since the compound nucleus formed is the same, the comparison gives a test of the predictions of Bohr's compound nucleus theory. The ratios of corresponding cross sections are in agreement with the compound nucleus theory. However, the excitation functions are displaced in energy by an amount not predicted by the theory. The disagreement is just outside of the experimental errors.

The excitation functions for reactions on various lead isotopes are found to be very similar. However, the excitation functions are found to be displaced in energy by an amount not equal to the differences in thresholds.

SYSTEMATICS OF EXCITATION FUNCTIONS WITH APPLICATION TO LEAD

Walter John, Jr.

Radiation Laboratory
University of California
Berkeley, California

August 4, 1955

I. GENERAL INTRODUCTION

Nuclear reactions in the medium-energy region (up to about 50 Mev bombarding energy) are commonly described by the statistical theory. The statistical theory is an elaboration of the compound-nucleus concept put forth by Bohr.[1] According to the compound-nucleus assumption a nuclear reaction proceeds in two stages: firstly the formation of a compound system and secondly the breakup of this compound system. The breakup and formation are independent processes. This concept can be reasonably justified in the region of isolated resonances. However, for the excitation energies obtaining in the medium-energy region, level widths are of the order of kev, level spacings of the order of ev. Hence there is a large overlapping of levels and the compound nucleus assumption cannot be rigorously made. Nevertheless, in order to make practical calculations for reactions, the compound-nucleus assumption is extended to the region of overlapping levels. The special assumptions of the statistical theory have been listed by Weisskopf.[2,3]

Ghoshal[4] devised a test of the applicability of Bohr's assumption to the medium-energy region. According to Bohr we may write a reaction

$$\sigma(a, b) = \sigma_c(a) G_c(b),$$

where $\sigma_c(a)$ is the cross section for formation of the compound nucleus C with the incident particle a and $G_c(b)$ is the probability of breakup of the compound nucleus with the emission of products b. $G_c(b)$ depends only on the excitation energy of C and not on the method of formation. We may then derive the following relation:

$$\frac{\sigma\ (a,b)}{\sigma\ (a,b')} = \frac{G_c(b)}{G_c(b')} = \frac{\sigma\ (a',b)}{\sigma\ (a',b')} .$$

Ghoshal bombarded Ni^{60} with 40-Mev α particles and Cu^{63} with 32-Mev protons. In both cases the resulting compound nucleus is Zn^{64}. The relation

$$\sigma(p,n):\sigma(p,2n):\sigma(p,pn) = \sigma(\alpha,n):\sigma(\alpha,2n):\sigma(\alpha,pn)$$

was observed to hold when 7 Mev was added to the proton energy to match the excitation energy of the compound nucleus. The prediction of Bohr's assumption was thus verified.

Calculations of the total cross sections for formation of the compound nucleus have been fairly successful.[2,3,5] The general features of these calculations may be illustrated by the expression

$$\sigma_c(a) = \pi \lambda\!\!\!^{-2}_a \sum_\ell (2\ell+1) P_{a\ell} \mathcal{E}_{a\ell} ,$$

where $\lambda\!\!\!^{-}_a$ is the reduced wave length of the incident particle a, ℓ the orbital angular momentum, $P_{a\ell}$ the penetration factor for the Coulomb and centrifugal barriers, and $\mathcal{E}_{a\ell}$ the "sticking factor" characterizing the interaction of the incident particle with the nucleus. The sticking factor is a pure number less than unity but approaching one at high energies. The gross behavior of the cross section depends on the penetration factor. For energies well below the barrier the W.K.B. approximation is used. Since the cross sections depend on the barrier height, they are sensitive to the value chosen for the nuclear radius. Comparison of experimental cross sections to calculated values have shown good agreement. Examples are $\sigma_c(p)$ for copper-63,[4] and bismuth-209,[6] $\sigma_c(\alpha)$ for rhodium-103,[3,8] silver-109,[3,8] bismuth-209,[6,7] nickel-60,[4] and others. An extensive series of (p,n) reactions were compared to the theory by Blaser, Boehm, Marmier, and Peaslee.[9]

The calculation of "partial" cross sections is more difficult and has been less successful. Blatt and Weisskopf[3] have given a detailed account of the statistical treatment. According to Bohr's assumption, the cross section $\sigma(a,b)$ for the reaction $X + a \rightarrow Y + b$ is written

$$\sigma(a,b) = \sigma_c(a) G_c(b).$$

By means of the reciprocity theorem, $G_c(b)$ may be written

$$G_c(b) = \frac{F_b}{\sum_c F_c} .$$

The sum is over all possible reaction products c, and

$$F_b = \sum_\beta k_\beta^2 \sigma_c(\beta).$$

The sum is taken over all channels β leading to the emission of b. Here k_β is the wave number corresponding to channel β. F_b may be written as an integral:

$$F_b(\mathcal{E}_{by}) = \frac{2M_\beta}{\hbar^2}\int_0^{\mathcal{E}_{by}} \mathcal{E}_\beta \sigma_c(\mathcal{E}_\beta)\, \omega_y(\mathcal{E}_{by}-\mathcal{E}_\beta)\, d\mathcal{E}_\beta .$$

The term $\sigma_c(\mathcal{E}_\beta)$ is the cross section for the formation of a compound nucleus from b and Y^* with channel energy $\mathcal{E}_\beta$. Y^* is the nucleus Y with the excitation energy $\mathcal{E}_{\beta y}-\mathcal{E}_\beta$; $\omega_y(\mathcal{E}_{by}-\mathcal{E}_\beta)$ is the level density of the nucleus Y^*. Unfortunately there is little knowledge, either experimental or theoretical, of level densities at the high excitation energies of interest here.

Weisskopf[2] and Blatt and Weisskopf[3] have developed a thermodynamic approximation to the level densities. A nuclear "temperature", θ, is defined

$$\theta(\mathcal{E}_{by}) = \frac{1}{\left(\frac{d\, \ln \omega}{d E}\right)_{E = \mathcal{E}_{by}}} .$$

The form of the level density is

$$\omega(E) = C\, e^{2\sqrt{aE}} ,$$

where C and a are constants. Rough calculations using various nuclear models yield similar level densities. Rough values of C and a have been given by Blatt and Weisskopf.[3] Presumably C and a should depend on the details of the nucleus in question. There is evidence that the density of levels in odd-odd nuclei is approximately four times that in even-even nuclei.[4,10,11] The study of inelastic proton scattering has shown some disagreement with the above form of the level density.[12,13]

On the basis of the evaporation theory Weisskopf[2] and Blatt and Weisskopf[3] have developed the following formulae for (a, n) and

(a, 2n) reactions:

below the (a, 2n) threshold, $\sigma(a, n) = \sigma(a)$;

above the (a, 2n) threshold and below the (a, 3n) threshold,

$$\sigma(a, 2n) = \sigma(a, n) \left[1 + \left(1 + \frac{\mathcal{E}_c}{\theta}\right) e^{-\frac{\mathcal{E}_c}{\theta}}\right].$$

Here $\mathcal{E}_c$ is the excess energy over the (a, 2n) threshold; θ is the temperature of the intermediate residual nucleus, that is, after evaporation of the first neutron has taken place. The evaporation formula for (a, 2n) reactions has been successfully fitted to the experimental data for $Rh^{103}(\alpha, 2n)$[8] and $Bi^{209}(p, 2n)$[6].

Although the statistical theory has had some success in describing reactions, many experimental data are accumulating that cannot be fitted by the statistical theory. The cross sections for the emission of charged particles are in many cases orders of magnitude greater than the statistical prediction.[14, 15, 16] Angular distributions of reaction products have been found to be strongly peaked forward instead of being symmetric around 90° in the center-of-mass system as predicted by statistical theory.[12, 17] These and other cases of serious disagreements with the statistical model indicate the need for caution in the application of the model to specific problems. The model may still yield useful information for certain regions of applicability.[13]

II. ALPHA-INDUCED REACTIONS ON LEAD

1. Introduction

The study of the alpha-induced reactions on lead is simplified by the fact that neutron emission is the predominant process. The emission of gamma rays is negligible by comparison, and the emission of charged particles is strongly depressed by the Coulomb barrier. For lighter target elements the emission of charged particles becomes important. For heavier elements fission competes with the other possible reactions.[18] The products of the (α, xn) reactions on lead are Po isotopes. The measurement of the Po alpha activities makes possible accurate determinations of absolute cross sections. Alpha-induced reactions on lead were studied by Templeton, Howland, and Perlman.[19] The Po products were studied but excitation functions were not made. Spiess[20] has measured excitation functions for Pb^{208} (α, n) and Pb^{208}(α, p).

The Pb^{206}(α, xn) reactions produce the compound nucleus Po^{210}, which is also the compound nucleus for the Bi^{209}(p, xn) reactions. The latter have been measured by Kelly.[6] Thus it is possible to make a comparison between the reactions to test the prediction of Bohr's assumption in the region of the heavy elements. The intercomparison of the numerous reactions on lead isotopes and the reactions for Bi + α and Bi + p yields information concerning the systematics of excitation functions for the heavy elements. The recent increase of the energy of the 60-inch cyclotron alpha beam makes it possible to study (α, 3n) reactions beyond their maxima and (α, 4n) reactions nearly to their maxima.

2. Study of the Reactions on Lead

In this experiment the excitation functions for (α, xn) reactions on lead were measured by bombarding stacked foils in the 48-Mev 60-inch cyclotron alpha beam. The induced Po alpha activities were identified and separated by pulse-height analysis, since some of the half lives are too long for decay analysis within a reasonable time. The reactions on the various lead isotopes were separated by the use of separated lead isotope targets. Experimental details are given in

Section III. Results are given in Section IV.

Table I lists the reactions and possible products. Table II lists the decay characteristics of the reaction products. The reactions on Pb^{204} were practically absent in the enriched isotope targets due to the very low abundance of Pb^{204}. The (α, γ) reactions are expected to give negligible interference due to the small cross section. The maximum observed cross section for $Bi^{209}(p, \gamma)$ was less than 1 mb.[6] The maximum cross sections of the (α, xn) reactions are of the order of 1 barn. All reactions leading to alpha emitters are contained in Table I. Only two involve proton emission. These are $Pb^{207}(\alpha, p)$ Bi^{210} and $Pb^{208}(\alpha, pn)$ Bi^{210}. Bi^{210} beta-decays into Po^{210}, an alpha emitter. The cross sections for these reactions were not measured in this experiment; however, they are expected to give little interference. Spiess[20] found the cross section for $Pb^{208}(\alpha, p)Bi^{211}$ to increase with increasing energy to 4 mb at the maximum energy of 39 Mev. Hence the $Pb^{207}(\alpha, p)$ Bi^{210} reaction is not expected to give appreciable interference here. Spiess also observed the excitation function for $Bi^{209}(\alpha, pn)Po^{211}$ (25-sec state only). The cross section increased with energy to 1 mb at 39 Mev. Templeton, Howland, and Perlman[19] found the cross section for $Pb^{208}(\alpha, pn)Bi^{210}$ to be 8 mb $\pm \sim 20\%$ at 40 Mev. It is therefore concluded that the reaction $Pb^{208}(\alpha, pn)$ Bi^{210} does not interfere below 40 Mev. From 40 to 50 Mev, however, it may increase to an appreciable fraction of the Po^{210} high-energy tail here attributed to $Pb^{208}(\alpha, 2n)Po^{210}$. All higher-order reactions have been neglected, since the cross sections are expected to be even smaller than those considered above. None of them leads to alpha emitters. Since their cross sections are small they do not appreciably affect the (α, xn) reactions through competition.

Table I

Reactions and products

Reaction	Reaction product for target nucleus:			
	Pb 204	Pb 206	Pb 207	Pb 208
(α, γ)	Po 208	Po 210	Po 211	Po 212
(α, n)	Po 207	Po 209	Po 210	Po 211
(α, 2n)	Po 206	Po 208	Po 209	Po 210
(α, 3n)	Po 205	Po 207	Po 208	Po 209
(α, 4n)	Po 204	Po 206	Po 207	Po 208
(α, 5n)	Po 203	Po 205	Po 206	Po 207
(α, p)	Bi 207	Bi 209	Bi 210	Bi 211
(α, pn)	Bi 206	Bi 208	Bi 209	Bi 210

Table II

Isotope table for reaction products[a] in Table I

Isotope	Type of Decay	Half life
Po 203	EC	47 m
Po 204	EC ~99%, α ~1%	3.8 h
Po 205	EC 99 + %, α 0.074%	1.5 h
Po 206	EC 96%, α 4%[b]	8.8d[c]
Po 207	EC 99 + %, α 1.4×10^{-2}%[b]	5.7 h
Po 208	α	2.93 y
Po 209	α ⩾90%, EC⩽ 10% est.	~100 y
Po 210	α	138.3 d
Po 211 (AcC')	α	0.52 s
Po 211	α	25 s
Po 212	α	3.04×10^{-7} s
Bi 206	EC	6.4 d
Bi 207	EC	~50 y
Bi 208	EC	long
Bi 209	stable	
Bi 210 (RaE)	β^- 99 + %, α 5×10^{-5}%	5.02 d
Bi 210	α, β^- or IT (~0.3%)	~10^6 y
Bi 211	α 99.68%, β^- 0.32%	2.16 m

[a] From Ref. 35 except where noted.

[b] Ref. 6.

[c] Half-life from this experiment.

III. EXPERIMENTAL METHODS

1. Preparation of Targets

The targets were made by evaporation of lead in vacuum onto 0.0005-inch 2SH aluminum foil backing. Foil blanks approximately 1/2 by 3/4 inch were stamped by a die. The bombarded portion was approximately 1/8 by 1/2 inch. The thickness of the lead deposit was about 1 mg/cm^2. It was measured to better than 1% by weighing on an assay balance. This thickness provided reasonable counting rates, kept self-absorption corrections small, and introduced negligible uncertainty in bombarding energy. Natural lead targets were made from high-purity lead (< 0.001% Bi). Evaporation was from a Mo filament at a distance of 18 inches from the foils.

Enriched lead isotope targets were prepared, with special precautions because of the limited quantity of the lead available. Table III gives the isotopic compositions of the leads used. The spectroscopic analyses showed chemical impurities to be negligible. The evaporation method was used to obtain the desired uniform density of lead on the targets. From consideration of the over-all accuracy of the experiment it was decided that the error from nonuniformity of the targets should not be much larger than 2%. This requires that the density of lead in the bombarded portion of the target should be within 2% of the mean density of the entire foil, the latter being determined by weighing.

The distance from the point of evaporation to the aluminum foil blanks was taken to be about 3 inches. This is the minimum distance that permitted the preparation of 35 foils simultaneously, or enough for one bombardment. To obtain uniform density of deposit on the foils, a curved foil holder was designed. The shape of the holder was determined by an approximate calculation. It was then found that the required shape could be approximated closely by a hemisphere 4.5 inches in diameter suspended with the center of the hemisphere 1.25 inches above the point of evaporation. The foil blanks were clamped to the inside of the holder. The holder was perforated where foil blanks could not be fitted together. A glass container was placed outside the holder to catch the lead isotope that escaped. This lead could then

Table III

Isotopic abundances of the target leads

Lead isotope	% of isotope			
	Natural lead	Enriched Pb^{206}	Enriched Pb^{207}	Enriched Pb^{208}
204	1.4	0.172	0.119	< 0.2
206	26.3	64.93	7.73	1.9
207	20.8	18.35	61.06	7.8
208	51.5	16.55	31.09	90.3

be recovered by dissolving it from the glass with acid. The holder was positioned over the cone with care, since the dimensions are fairly critical. Each evaporation required 300 mg of lead isotope to obtain a density of ~1 mg/cm^2 on the foils. Approximately 30% of the lead was deposited on the foils, 20% on the target holder and 50% on the glass (from which it could be recovered).

Evaporation of the lead took place from a small graphite cone with an included angle of 120°. This was slightly larger than the angle subtended by the entire foil holder. The cone was made of high-purity graphite and was heated white-hot in vacuum to drive off volatile impurities. The cone was heated by electron bombardment from a surrounding filament. Heat shielding protected the foils from heat radiated by the filament. The lead for the evaporation formed a small bead in the bottom of the cone. Trial evaporations were made with ordinary lead. First trials gave a dark-colored deposit. This was attributed to heating effects due to the proximity of the foils to the hot cone. In later evaporations the temperature of the cone was maintained low enough that it required about thirty minutes for the lead to evaporate. The deposit obtained was shiny and adherent. Variation in lead density on adjacent foils averaged two or three percent. Thus the foils were acceptable for bombardment. Variation in the absolute density of deposit for different regions of the holder was somewhat larger. This, however, does not affect the accuracy of the experiment.

The enriched Pb^{206} and Pb^{207} leads were supplied in the form of the monoxide. The monoxide was reduced to metallic lead by heating it in a hydrogen atmosphere. The reduction was carried out in a graphite cone. The metallic lead collected as beads. Weighings showed that the reduction was complete. The enriched Pb^{208} was supplied as the chloride. This was first converted to the oxide and then reduced.

2. Bombardment

Bombardments were carried out with the 60-inch cyclotron in Crocker Laboratory. Alpha particles with energies up to 48 Mev were used. The energy spread of the external beam was reduced by allowing it to travel about 3 feet in the fringing magnetic field of the

cyclotron magnet. The beam traveled in a tube connected to the cyclotron vacuum system with 1/8-inch-wide collimating slits at front and back.* The tube was hinged in the middle and could be aligned on the beam by remote control. Two foil wheels containing absorbers and the target were located on the end of the tube. A Faraday cup was placed behind the foil wheels to measure the transmitted beam. Figure 1 is a schematic diagram of the target apparatus. Figure 2 is a photograph of the target assembly in place at the 60-inch cyclotron.

The beam energy was determined from the mean range of the alpha beam in aluminum. Figure 3 is a typical range curve. Ranges in aluminum were converted to energy by means of the experimental range-energy relation of Bichsel and Mozley.[21, 22, **] The target foils were bombarded in stacks with the lead film facing the beam. Ranges in the target stacks were calculated to the center of each lead film. The lead thickness was converted to aluminum equivalent with the aid of the range-energy tables of Aron, Hoffman, and Williams.[24] The stopping-power ratios obtained were compared to those experimental values for the stopping-power ratio of bismuth to aluminum which were measured by Kelly.[25] The agreement was good; moreover, the conversion is insensitive to inaccuracies of the relative stopping power, since the lead films are thin.

An effort was made to maintain constant those cyclotron parameters affecting the beam energy. The target assembly was operated by remote control so that the beam need not be turned off and on with consequent uncertainties in energy. The range of the beam was observed to drift somewhat during the cyclotron warm-up period. A range curve was taken just before bombardment, the target was bombarded for about ten hours, and a range curve was taken after bombardment. The drift in range during bombardment was generally less than

---

* The apparatus is an improved version of that used by Kelly[6] and Kelly and Segrè[7].

** For a given energy, the range from Bichsel and Mozley's experiments is about 1.2% higher than the theoretical values of Smith.[23]

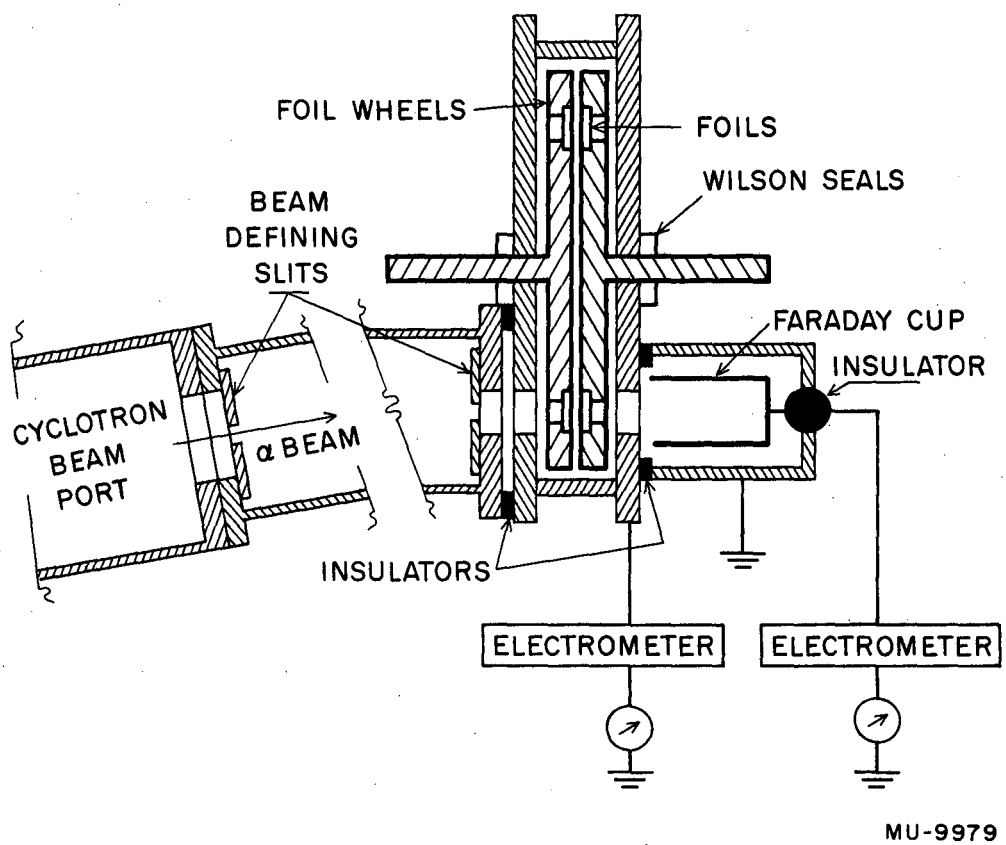

Fig. 1. Schematic diagram of the target apparatus.

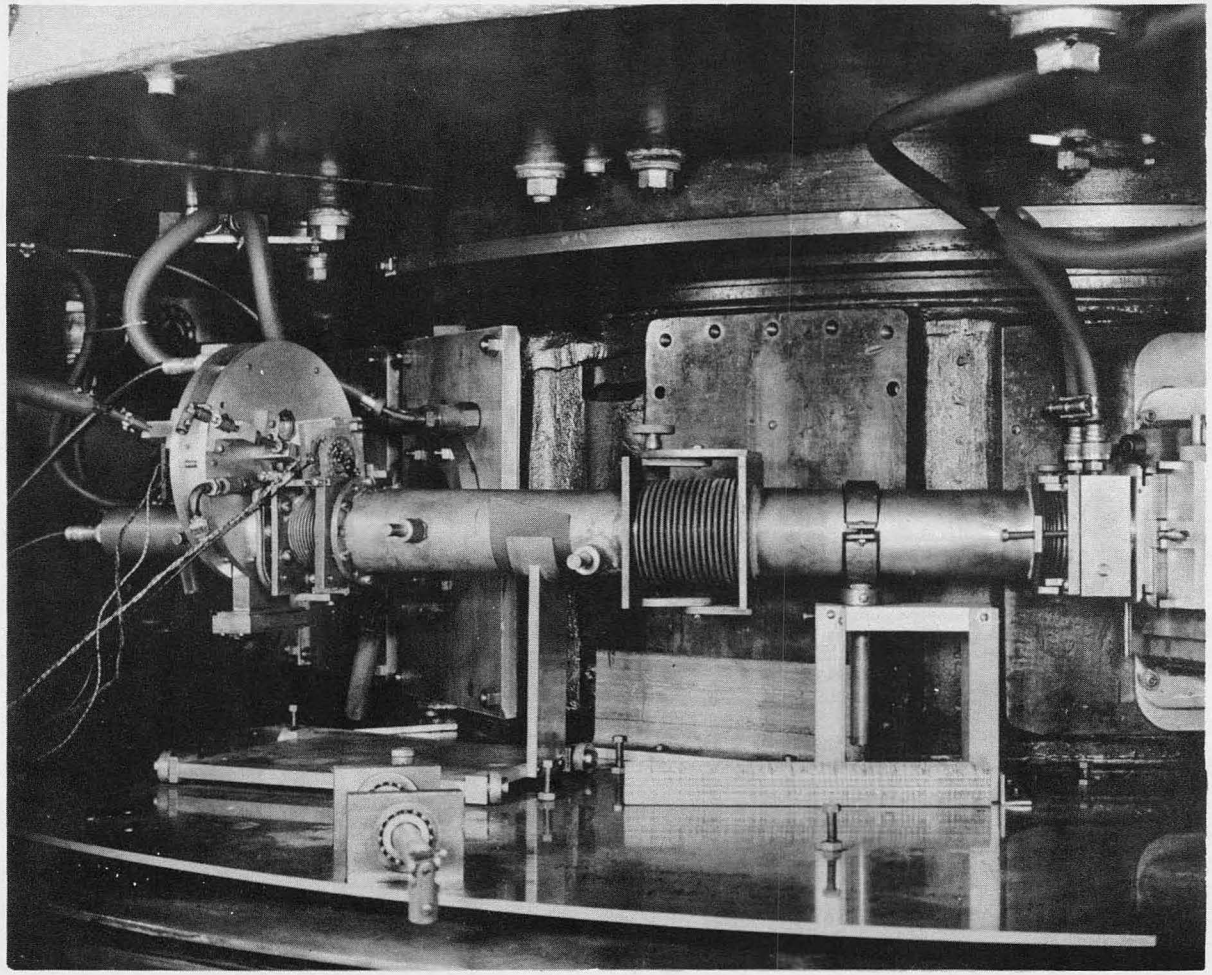

ZN-1348

Fig. 2. Target assembly in place at the 60-inch cyclotron.

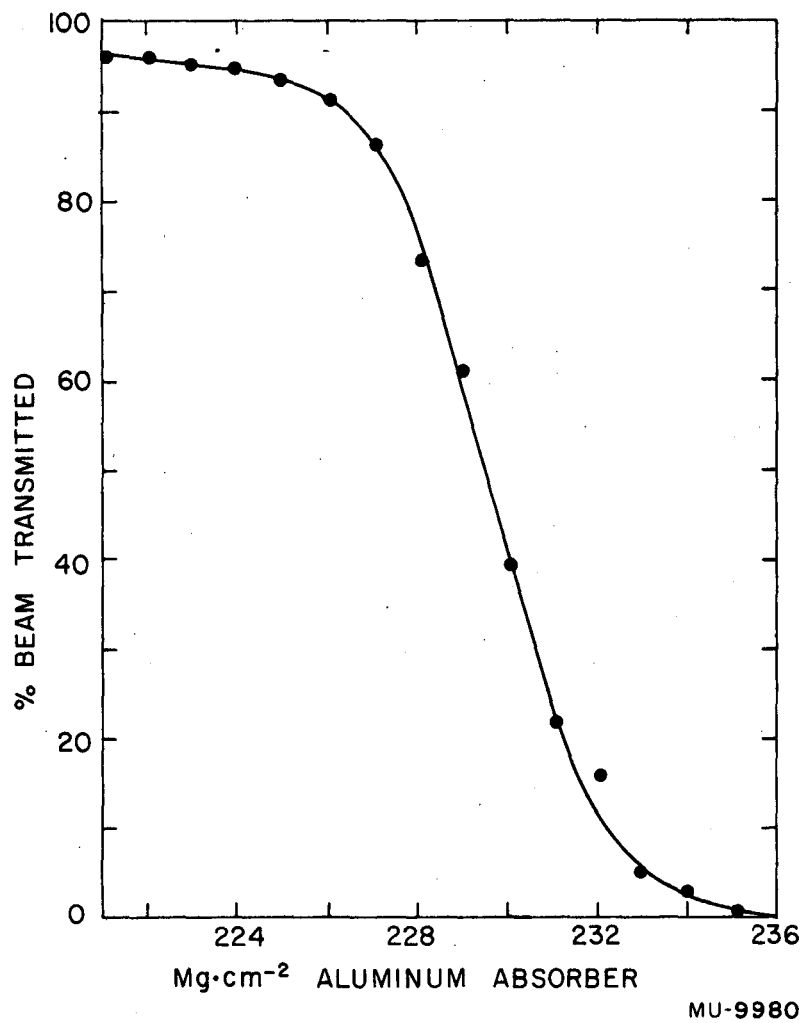

Fig. 3. Typical range curve of 60" cyclotron alpha beam.

1 mg/cm^2 Al. Both the beam stopping on the foil wheel and the beam transmitted to the Faraday cup were monitored. This made range determinations independent of beam intensity, which fluctuated during bombardment. Range straggling of the beam was $\frac{R_{extr.} - R_o}{R_o} = 1.2\%$, where $R_{extr.}$ is the extrapolated range and R_o is the mean range. The theoretical range straggling in Al^{26} is 0.9%.

The beam current was kept at about 0.1 μamp. It was found that higher beam levels caused heating damage to the lead foils. The beam was integrated with University of California Radiation Laboratory feedback-type electrometers, using a 1-μfd input capacitor. The capacitor was automatically discharged at a preset voltage and the output traced on a Speedomax recorder. The integrating capacitor was calibrated to 0.2% on an impedance bridge. As a further check the capacitor was compared to a Bureau of Standards $10^8 \Omega$ resistor by alternating them in the input curcuit with a constant-current input. The relative values agreed to within 0.5%. The over-all calibration of the electrometer system was checked by measuring an accurately known current. This current was generated by placing a Leeds and Northrup potentiometer voltage in series with the Bureau of Standards resistor. The output of the electrometer was found to be 1.5% low. This is a reasonable correction, since the voltage dividing network at the output consists of several 1%-tolerance resistors.

Secondary electron emission from the Faraday cup was suppressed by the strong fringing field of the cyclotron magnet. The vacuum was essentially that of the cyclotron tank, eliminating possible errors from gas ionization. The Faraday cup, foil wheel, and associated cables were checked for current leakage. The cup (or wheel) was attached to the input capacitor of the electrometer and charged up with a dummy current source. No detectable leakage was observed in periods as long as 15 minutes. In operation, the capacitor is discharged every two or three minutes. The Faraday cup was checked for leakage under actual bombardment conditions by charging it up with the beam and then isolating it by stopping the beam on the foil wheel. Checks were also made to insure that rf pickup was negligible. The battery-operated electrometers were warmed up overnight. No

appreciable drifting of the zero point was observed during the bombardments.

3. Counting

Gross alpha counting was done with UCRL ZnS-5819 scintillation counters and scalers. The sample slide positioned the active foils to a point about 1/16 inch below the ZnS screen. Counting rates ranged up to about 15,000 cpm. The scintillation counters were calibrated by comparison to a 2π-geometry ionization chamber. The ionization chamber was 1.5 cm deep and was filled with argon at 1.7 atmos. The counting efficiency of the scintillation counters was found to be 97% of that of the ionization chamber. The counting efficiency of the ionization chamber was taken to be 50%. Corrections for self-absorption and back scattering were made by the methods of Rossi and Staub.[27] Typical corrections to observed counting rates were + 3.5% to account for self-absorption and -1% for back scattering. The scintillation counters had broad plateaus and were essentially free from background. In addition, samples could be changed more rapidly than with an ionization chamber. An alpha standard was counted periodically. The observed counting rate remained constant to within 1%.

Gross alpha activities were followed up to the time of the pulse analysis. The time from bombardment to pulse analysis varied from a few weeks to a few months. Decay corrections for Po^{208}, Po^{209}, and Po^{210} introduced negligible uncertainty in the results because of the long half lives and the accuracy to which they are known. The shorter-lived Po^{206} and Po^{207} are discussed in Section IV.

The Polonium isotopes 206, 208, 209, and 210 were identified and their relative abundance determined by alpha pulse-height analysis. The sample was placed in a gridded ionization chamber; the output pulses were fed into a 48-channel pulse-height analyzer.[28] The alpha counts of each isotope were thus separated according to the energy of the alpha particles. The plot of a typical pulse-height analysis is shown in Fig. 4. The extremely thin samples required for the pulse-height analysis were prepared by dissolving the targets in HNO_3, boiling with HCl to destroy the nitrate, and plating onto Ag blanks by

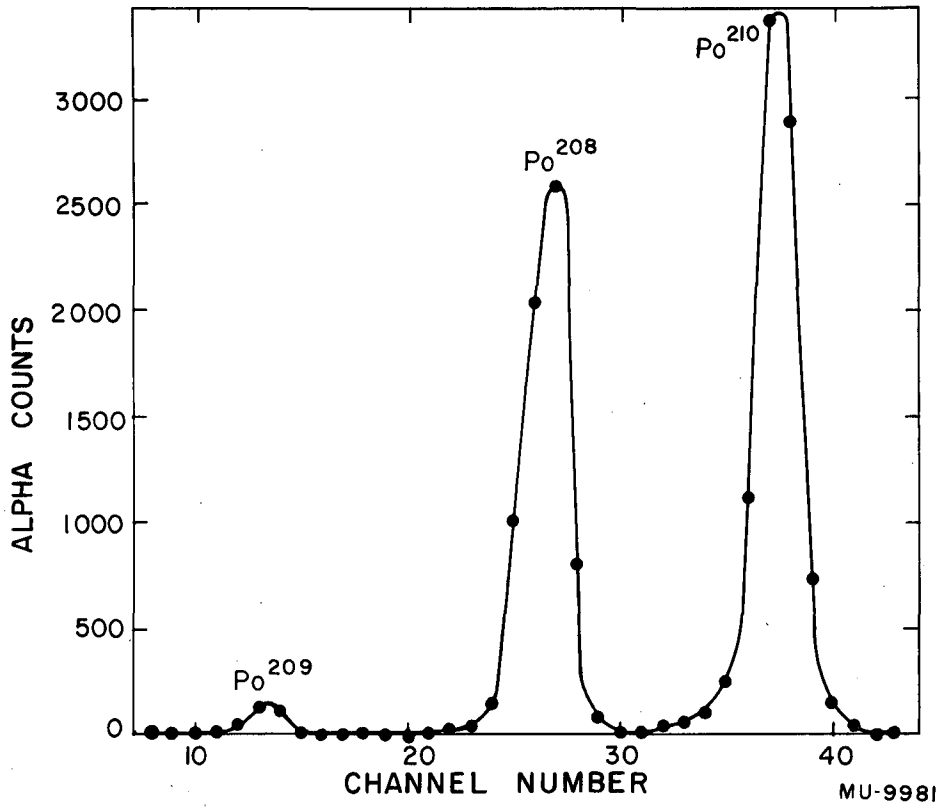

Fig. 4. Plot of an alpha pulse height analysis to illustrate the measurement of the relative abundances of the polonium isotopes.

electrodeposition. The chemistry of each sample was carried out in new glassware. In addition, blanks were carried through the chemistry as a precaution against cross-contamination. With care, it was found possible to plate out a desired amount of activity to within ± 25%. The amount plated out was controlled in order to control counting losses in the analyzer. Register losses are the principal source of these counting losses. The samples ranged from 100 to 1000 cpm, depending on the relative percentages of the isotopes present and the desired accuracy. Sample rates were adjusted so that the statistical error would be larger than the register losses in most cases. Test analyses of samples with various counting rates indicated no serious deviations from statistical errors. For the natural lead targets every other sample was analyzed. All the enriched isotope samples were analyzed.

Decay analysis was applied to the alpha activities of Po^{206} and Po^{207}. In addition, the gamma activities of these two isotopes were counted with a NaI scintillation counter having a cylindrical crystal 1.5 by 1 inch. For Po^{207} the relative gamma activity was more accurately determined than the relative alpha activity, owing to the extremely small alpha-branching ratio. Therefore relative cross sections for Po^{207} were based on the gamma counting. The absolute values of the cross sections were normalized to the alpha counting.

Aluminum blanks were spaced throughout the target foil stacks. These blanks were counted to detect any activity induced in the aluminum or its impurities. The use of blanks also checked against the possibility of transfer of activity from the lead foils by recoil or from handling. No alpha activity was found on any of the blanks. The aluminum did show some gamma activity. This background activity was subtracted from the gamma activity of the lead foils.

The over-all operation of the equipment was checked by a trial bombardment of bismuth. A few points were obtained on the excitation function $Bi^{209}(\alpha, 2n)At^{211}$. These agreed well with the data of Kelly and Segrè.[7]

IV. RESULTS

1. Measured Cross Sections

Tables IV to VI give the cross sections calculated from the data of this experiment. The excitation functions are plotted in Figs. 5, 6, and 7. The cross-section measurements for the enriched isotopes were made at intervals of approximately 1 Mev. So that the results of the various bombardments could be combined, the cross sections were interpolated graphically to integral numbers of Mev. The error introduced by the interpolation was smaller than the uncertainties of the measurements.

2. Errors in the Cross Sections

The errors shown on the graphs and listed in Table VII are estimated relative errors. These were calculated from the counting statistics of the pulse analysis and gross counting with an additional 2% error for nonuniformity of the isotope targets.

In addition to the relative errors, the error in absolute value of the cross sections is estimated to be ± 3%. The factors contributing to this error are assessed as follows:

capacitor dumping accuracy and electrometer drift	± 1%
capacitor calibration	± 0.5%
electrometer calibration	± 1%
ion chamber efficiency	± 1%
ion chamber bias correction	± 1%
relative efficiency of ZnS counters	± 1%
backscattering and self-absorption correction	± 1%

Thus the total error of the most accurate cross sections is about 3.5%.

The cross sections calculated from the enriched-isotope data were combined and compared with the natural-lead results for the production of the various Po isotopes. Good agreement was obtained in magnitude and energy dependence. The yield of Po^{210} from natural lead was about 4% higher than calculated from the $Pb^{208}(\alpha, 2n)Po^{210}$ and $Pb^{207}(\alpha, n)Po^{210}$. (The problem of interference between various reactions was discussed in Sec. II, 2.)

Table VI

Cross section in barns for the reaction
$Pb^{208}(\alpha, 3n)Po^{209}$

Alpha Energy (Mev)	Cross Section (barns)
30.3	0.0
31.0	0.3
31.6	0.7
32.9	0.4
34.1	0.8
34.7	0.8
35.9	1.1
37.1	0.9
38.2	0.9
39.3	1.0
40.3	1.1
41.4	0.8
42.4	1.0
43.4	0.7
44.4	0.5
45.3	0.8
46.2	0.6
47.1	0.5

Table V

Cross sections for the production of Po^{206}, Po^{208}, Po^{209} and Po^{210} by alpha-particle bombardment of natural lead. $\sigma_j = \sum_i a_i \sigma_{ij}$ are listed where a_i is the fractional abundance of lead isotope i and σ_{ij} is the cross section in barns for production of polonium isotope j from lead isotope i. The σ_j are from direct measurements.

Alpha Energy (Mev)	Po 208 Run I (barns)	Po 208 Run II (barns)	Po 208 Run III (barns)	Po 209 Run I (barns)	Po 209 Run II (barns)	Po 209 Run III (barns)	Po 210 Run I (barns)	Po 210 Run II (barns)	Po 210 Run III (barns)	Po 206 Run III (barns)
18.3				0.001			0.0014			
19.1		0.0002			0.004			0.0058		
19.3	0.0002			0.004			0.0057			
20.3	0.0004			0.018			0.0167			
20.4		0.0006			0.02			0.020		
21.3	0.004	0.004		0.030	0.04		0.046	0.049		
22.2	0.014	0.016		0.06	0.07		0.090	0.099		
23.0	0.040			0.11			0.156			
23.1		0.045			0.11			0.168		
23.9	0.074			0.16			0.220			
24.7		0.104			0.12			0.283		
24.8	0.102			0.09			0.278			
25.5		0.137			0.14			0.345		
25.6	0.132			0.13			0.330			
26.4	0.152			0.15			0.375			
27.1		0.19			0.17			0.43		
27.2	0.20			0.21			0.44			
27.8		0.21			0.19			0.47		
28.0	0.22			0.20			0.50			
28.7	0.23			0.21			0.51			
29.2		0.24			0.22			0.52		
29.5	0.24			0.25			0.54			
30.0		0.26			0.28			0.54		
30.2	0.26			0.34			0.56			
30.7		0.27			0.33			0.54		
30.9	0.29			0.35			0.54			
31.4		0.31			0.39			0.50		
31.6	0.34			0.31			0.51			
32.1		0.34			0.43			0.44		
32.3	0.36			0.47			0.44			
32.8		0.31			0.41			0.33		
32.9	0.37			0.55			0.371			
33.4		0.36			0.49			0.318		
33.6	0.38			0.53			0.318			
34.2	0.38			0.47			0.269			
34.6		0.36			0.53			0.229		
34.8	0.36			0.53			0.219			
35.5	0.38			0.56			0.186			
35.8		0.34			0.52			0.160		
36.2	0.36			0.60			0.156			
36.8	0.36			0.56			0.133			
37.0		0.39			0.56			0.127		
37.5	0.36			0.58			0.117			
37.8			0.36			0.61			0.107	
38.1	0.37			0.57			0.102			
38.2		0.36			0.58			0.100		
38.7	0.40			0.68			0.099			
38.9			0.37			0.67			0.090	0.02
39.3		0.39			0.64			0.086		
39.9			0.41			0.65			0.078	0.05
41.0			0.45			0.58			0.070	0.08
41.9			0.50			0.44			0.065	0.17
42.9			0.56			0.50			0.062	0.33
43.9			0.63			0.31			0.057	0.50
44.8			0.62			0.26			0.055	0.70
45.8			0.72			0.21			0.053	0.89
46.7			0.72			0.26			0.045	1.11
47.7			0.75			0.25			0.049	1.21
48.6			0.76			0.30			0.046	1.30

Table VI

Cross section in barns for the reaction
$Pb^{208}(\alpha, 3n)Po^{209}$

Alpha Energy (Mev)	Cross Section (barns)
30.3	0.0
31.0	0.3
31.6	0.7
32.9	0.4
34.1	0.8
34.7	0.8
35.9	1.1
37.1	0.9
38.2	0.9
39.3	1.0
40.3	1.1
41.4	0.8
42.4	1.0
43.4	0.7
44.4	0.5
45.3	0.8
46.2	0.6
47.1	0.5

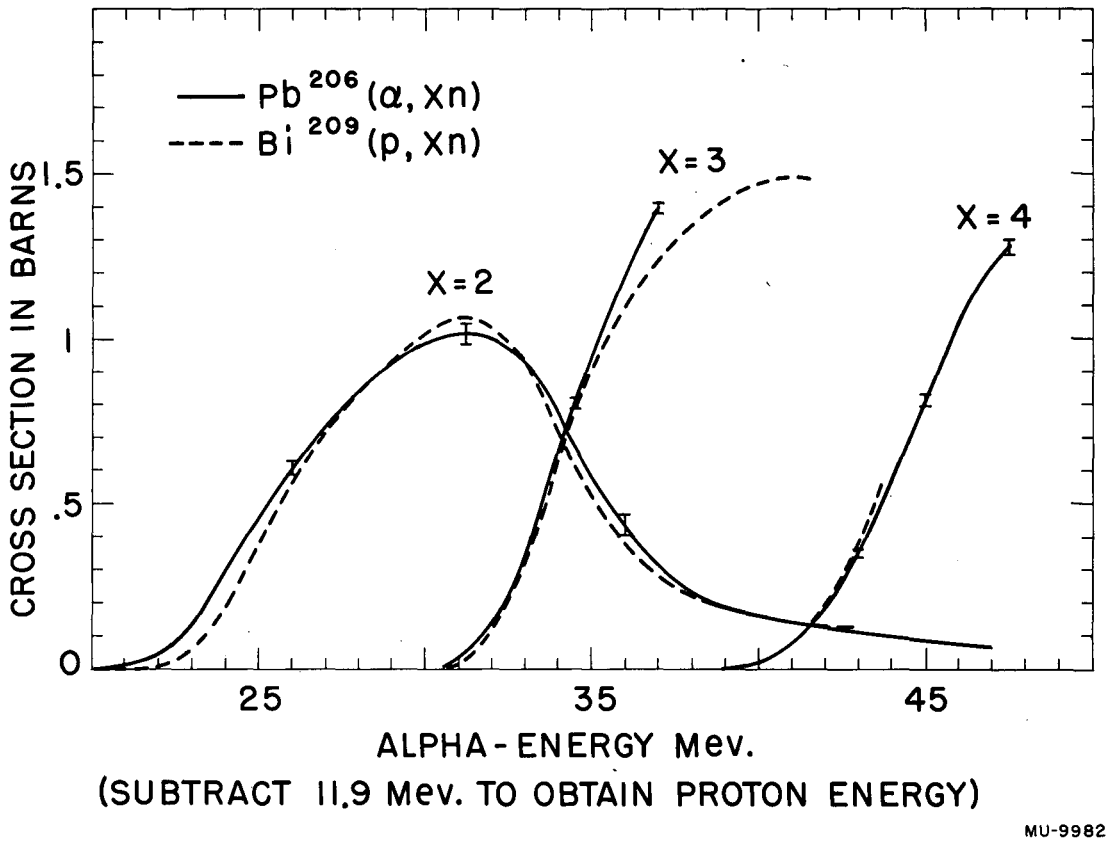

Fig. 5. Comparison of the excitation functions of Pb^{206} + α and Bi^{209} + p. Bi data taken from Ref. 6.

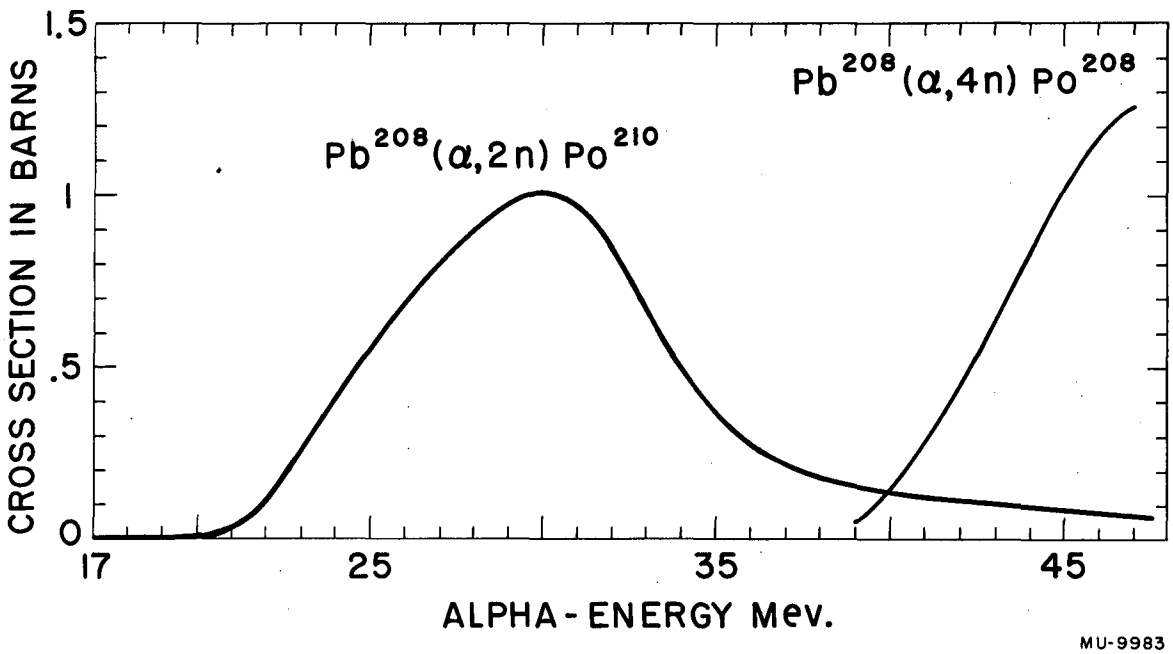

Fig. 6. Excitation functions for Pb^{208} (α, 2n) Po^{210} and Pb^{208} (α, 4n) Po^{208}.

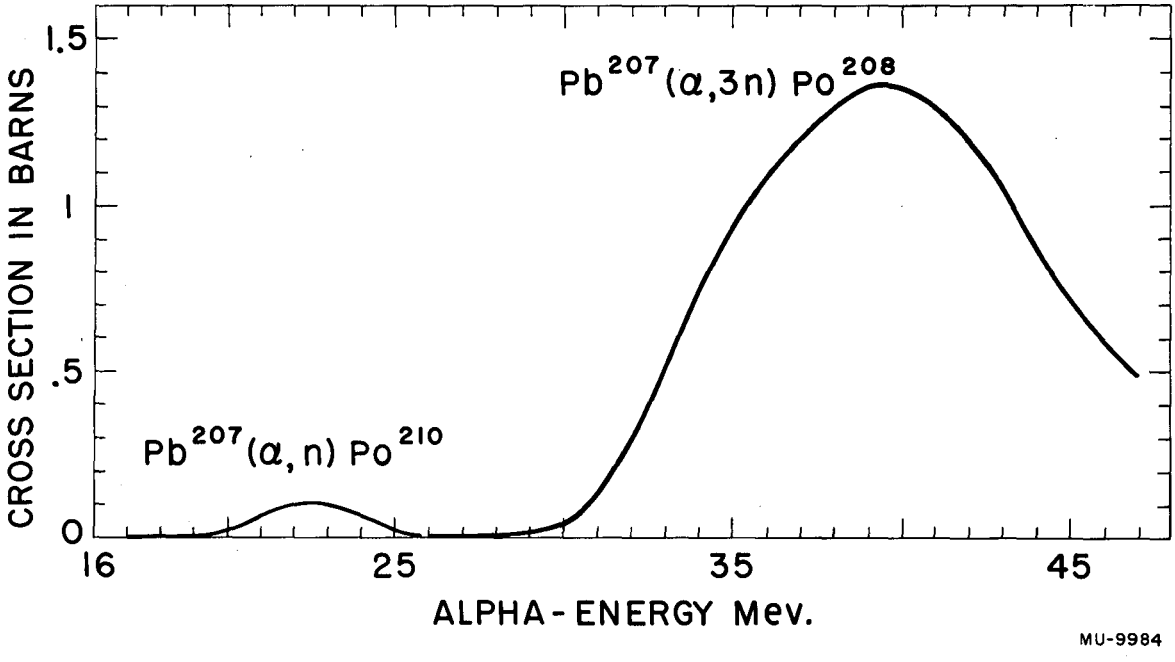

Fig. 7. Excitation functions for Pb^{207} (α, n) Po^{210} and Pb^{207} (α, 3n) Po^{208}.

Table VII

Estimated relative errors in the cross sections

Reaction	Energy (Mev)	Error (barns)	% error
$Pb^{206}(\alpha, 2n)Po^{208}$	21	0.002	15
	22	0.002	5
	26	0.02	3
	31	0.03	3
	35	0.03	5
	38	0.02	9
	42	0.02	13
	46	0.02	24
$Pb^{206}(\alpha, 3n)Po^{207}$	32	0.006	4
	35	0.02	2
	37	0.03	2
	39	0.04	2
$Pb^{206}(\alpha, 4n)Po^{206}$	40	0.007	100
	43	0.01	3
	45	0.02	2
	47	0.03	2
$Pb^{207}(\alpha, n)Po^{210}$	20	0.0007	3
	22	0.004	4
	23	0.006	6
	24	0.008	11
	25	0.01	33
$Pb^{207}(\alpha, 3n)Po^{208}$	27	0.009	180
	31	0.01	10
	34	0.02	3
	36	0.03	3
	40	0.04	3
	44	0.04	4
	46	0.04	6
$Pb^{208}(\alpha, 2n)Po^{210}$	20	0.0002	3
	22	0.002	2
	25	0.01	2
	30	0.02	2
	35	0.01	3
	40	0.004	3
	45	0.005	5
$Pb^{208}(\alpha, 4n)Po^{208}$	38	0.01	40
	40	0.01	7
	42	0.02	4
	44	0.03	3
	46	0.03	3

The energies for the lead bombardments are estimated to be correct within ± 0.2 Mev, allowing for observed drifts of the cyclotron energy. The intercomparison of excitation functions present in several bombardments supports this conclusion.

3. Yields of Po^{206}, Po^{207}, and Po^{209}

The cross sections for $Pb^{206}(\alpha, 3n)Po^{207}$ and $Po^{206}(\alpha, 4n)Po^{206}$ depend on the alpha branching ratios of Po^{207} and Po^{206}. The values used here are from Kelly.[6] The uncertainty of these branching ratios is larger than the errors discussed above.

The Po^{206} yields could be determined in three ways. One depended largely on the pulse analysis, the second depended largely on decay analysis. The third was from the relative yields given directly by the gamma counting. All three showed excellent agreement. The half life of Po^{206} has been determined to be 8.8 ± 0.1 days. A decay curve is plotted in Fig. 8.

The decay data of Kelly[29] were reanalyzed to check the half life of Po^{207}. The value computed was 6.2 ± 0.1 hours, compared to 5.7 hours found by Templeton, Howland, and Perlman.[19] However, the effect on the calculated cross section was found to be negligible. As a check on the beam integration the bombardment period was divided into hourly intervals. After decay corrections were made the final result was within 2% of the result for constant beam current. The absolute normalization of the reaction $Pb^{206}(\alpha, 3n)Po^{207}$ is uncertain by ± 6%, owing largely to alpha counting statistics. The reaction $Pb^{206}(\alpha, 3n)Po^{207}$ was not calculated above 37 Mev because of the interference from the reaction $Pb^{206}(\alpha, 4n)Po^{206}$.

The half life for Po^{209} was taken to be 100 years.[6] The uncertainty is about ± 50 years. Because of the long half life, counting statistics were relatively poor. No attempt was made to calculate the excitation functions for $Pb^{206}(\alpha, n)Po^{209}$ and $Pb^{207}(\alpha, 2n)Po^{209}$.

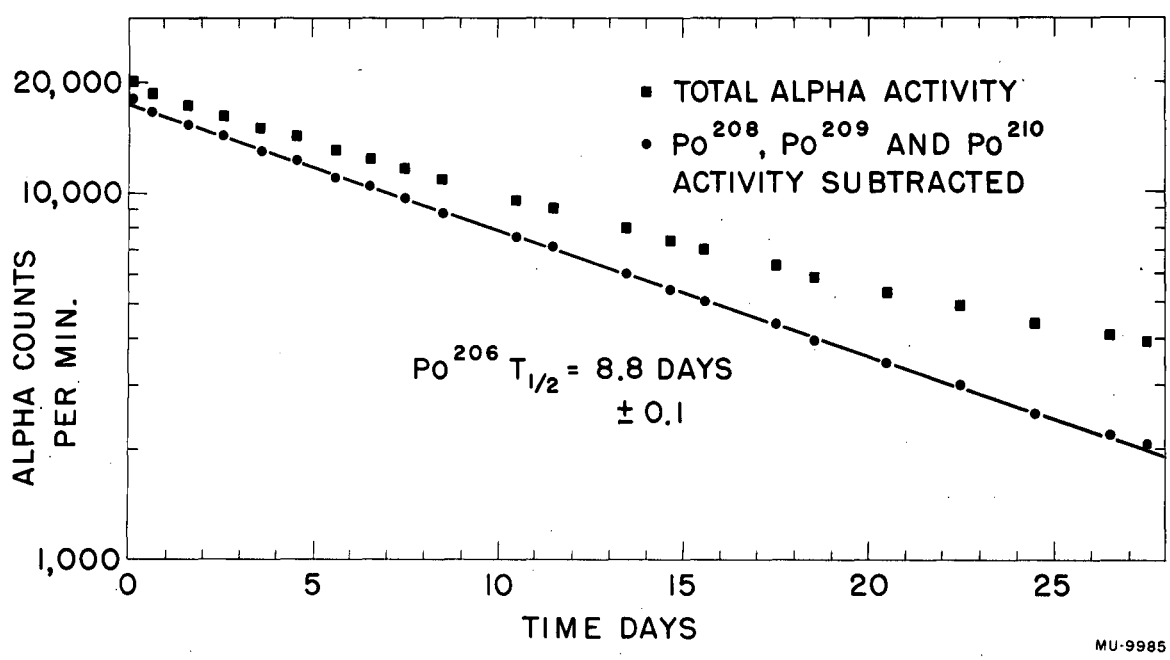

Fig. 8. Alpha decay curve for Po^{206}.

V. DISCUSSION

1. Test of the Predictions of Bohr's Compound Nucleus Theory

The comparison between the excitation functions for $Pb^{206} + \alpha$ and Bi + p is illustrated in Fig. 5. The compound nucleus produced in both cases is Po^{210}. The proton curves have been shifted by adding 11.9 Mev to the proton energy in order to match the curves. In order to satisfy the prediction of Bohr's theory it must be possible to shift the curves so that

$$\sigma(p, 2n) : \sigma(p, 3n) : \sigma(p, 4n) = \sigma(\alpha, 2n) : \sigma(\alpha, 3n) : \sigma(\alpha, 4n).$$

Inspection of Fig. 5 reveals that this condition is well satisfied. However, the compound nucleus theory requires that the curves be shifted by an amount which would produce the compound nucleus with the same excitation energy. The transformation from center-of-mass coordinates to laboratory coordinates must be made in calculating the exact energy shift required. The relation between the proton and alpha energies in the center-of-mass system must be

$$E_p^{c.m.} = E_\alpha^{c.m.} - \Delta Mc^2$$

where $\Delta M = M_{Bi} + M_H - M_{Pb^{206}} - M_{He}$.

In the laboratory system,

$$\frac{209}{210} E_p = \frac{206}{210} E_\alpha - \Delta Mc^2$$

or $E_p = a E_\alpha - b$

where $a = \frac{206}{209}$, and $b = \frac{210}{209} \cdot \Delta M c^2$.

The value of b found by matching the experimental curves is 11.3 ± 0.4 Mev. The transformation of coordinates introduced a correction of about 0.6 Mev. The uncertainty is estimated from the uncertainties in the bombarding energies. Kelly[6] estimated the error in the proton bombardment energies for the Bi + p experiments to be ± 0.3 Mev. Kelly experienced some difficulty in determining the beam energy of the linear accelerator but found good agreement between several bombardments. The alpha bombardment energies are considered to be accurate to ± 0.2 Mev. This error was estimated from observed drifts in the cyclotron energy. An internal check was

also made between all the lead bombardments. Since the targets were not completely separated isotopes, some reactions were visible in all targets. The excitation functions for these reactions could be compared to test the energy determinations. The reactions $Pb^{206}(\alpha, 4n)Po^{206}$ and $Pb^{208}(\alpha, 2n)Po^{210}$ were especially useful for this purpose. The intercomparisions supported the above estimate of the error in bombardment energy.

We note that the comparison between the lead and bismuth cross sections is independent of the uncertainty in the alpha branching ratios of Po^{206} and Po^{207} since the same values were used in both calculations. For the comparison the proton ranges were converted to energy using the Bichsel and Mozley[21] range-energy table. The correction to the energies from the Smith[23] range-energy table is small however.

We now calculate b from the masses. We note that ΔM contains the difference between the Bi^{209} and Pb^{206} masses. This difference may be taken from the table of Stern[30] or the more recent table of Glass, Thompson, and Seaborg.[31] The latter table is based on a different value for the Pb^{208} mass thereby altering the normalization of the masses. However, the mass difference needed here is the same in both tables. The mass tables in the region of lead are based on decay energies and neutron binding energies. For example, we may link Bi^{209} and Pb^{206} as follows:

$$Pb^{206} \xrightarrow[\text{6.73 Mev B.E.}]{+\,n^{o}} Pb^{207} \xrightarrow[\text{7.38 Mev B.E.}]{+\,n^{o}} Pb^{208} \xrightarrow[\text{3.87 Mev B.E.}]{+\,n^{o}} Pb^{209} \xrightarrow[\text{0.64 Mev}]{\beta^{-}} Bi^{209}$$

The data is taken from Glass, Thompson, and Seaborg. All of the energies listed are measured energies. The difference in mass values is estimated to be accurate to ± 0.1[31] or ± 0.2 Mev.[30] The value of b calculated from the mass values is 10.5 ± 0.2 Mev.

The calculated value of b, 10.5 ± 0.2 Mev, is to be compared to the experimental value of 11.3 ± 0.4 Mev. The experimental value thus appears to be higher than the calculated value by 0.8 ± 0.5 Mev, or by an amount just outside of the probable error. Because of this suspected disagreement with theory the Ghoshal[4] experiment has been

reexamined. Ghoshal compared the excitation functions for $Cu^{63} + p$ and $Ni^{60} + \alpha$. He found that the excitation functions could be matched by shifting the proton curves by 7 ± 1 Mev. This shift does not take into account the transformation from center-of-mass to laboratory coordinates. Because of the lighter elements involved here the correction is greater than for the lead-bismuth case. In the laboratory system the energies are again related by

$$E_p = a\,E_\alpha - b$$

$$\text{where } a = \frac{60}{63}\ ,\quad b = \frac{64}{63}\ \Delta M\, c^2$$

$$\text{and } \Delta M = M_{Cu63} + M_H - M_{Ni60} - M_{He}\ .$$

We note that the proton curves are stretched by 1.3 Mev more at the highest energies relative to the lowest energies. The value of b found to fit the experimental curves is 6.4 ± 1.0 Mev. The uncertainty is taken from Ghoshal's estimate. The value of b for Ghoshal's experiment may be calculated from the masses taken from the table of Bainbridge.[32] The result is b = 3.2 ± 0.3 Mev. The difference between the observed and calculated b is 3.2 ± 1 Mev. This difference is therefore considered to be outside of the errors involved. In both the Cu-Ni and Bi-Pb comparisons the observed b is larger than the b calculated from the masses. The discrepancy is greater for the Cu-Ni comparison.

The reason for the discrepancy between the observed and calculated energy shift b is not clear. It is not explained by the compound nucleus-statistical theory. In fact, the explanation is likely to involve a non-compound nucleus process. The observed behavior of the excitation functions for the reactions on a given target nucleus shows competition between the processes involving the emission of one to four neutrons. Furthermore, the ratios of the cross sections for reactions producing the same compound nucleus satisfy the prediction of Bohr's theory if a suitable energy shift is employed. We are therefore led to suspect that the initial stage of the encounter between the proton and its target nucleus or between the alpha particle and its target is at least partially a non-compound nucleus process. After this initial stage a compound nucleus is formed,

and the evaporation of successive neutrons proceeds in a statistical manner. If during the initial stage the first neutron emitted in the proton-induced reaction has on the average more energy than the first neutron emitted in the alpha particle-induced reaction the energy discrepancy may be accounted for. There is considerable evidence for non-compound nucleus processes. The complex-potential model of the nucleus[33] is based on experimental evidence that a neutron incident on a nucleus may travel an appreciable distance inside the nucleus without forming a compound nucleus. A proton might enter a nucleus and eject a neutron by a direct interaction. Furthermore, the energy of the ejected neutron would be different for an incident proton than for an incident alpha particle. There is also experimental evidence for interactions with the diffuse rim of the nucleus.[17] An interaction with the diffuse rim resulting in ejection of a neutron would be different for an incident proton than for an incident alpha particle. The arguments presented here are intended only as suggested explanations. A quantitative account of the discrepancy between the observed and calculated value of b may be possible only when a more detailed theory of nuclear reactions becomes available.

2. General Features of the Excitation Functions in the Region of Lead

The alpha bombarding energies ranged from about 20 Mev to 47 Mev. In this energy region the number of neutrons observed to be emitted in reactions on lead increases from one to four as the energy increases. A slight indication of the beginning of the reaction $Pb^{207}(\alpha, 5n)Po^{206}$ was seen at 47.5 Mev. The excitation functions exhibit a characteristic competition between the reactions involving the emission of various numbers of neutrons. The excitation functions for reactions on the various lead isotopes are very similar. They are also similar to the excitation functions for alpha and proton bombardment of bismuth.

In Fig. 9 all of the available excitation functions for lead and bismuth have been graphed for comparison. The energy scale is that for $Pb^{206} + \alpha$. The energy scales for the other excitation functions have been shifted to give a visual match of apparent thresholds. The observed shifts and the shifts calculated from mass values available

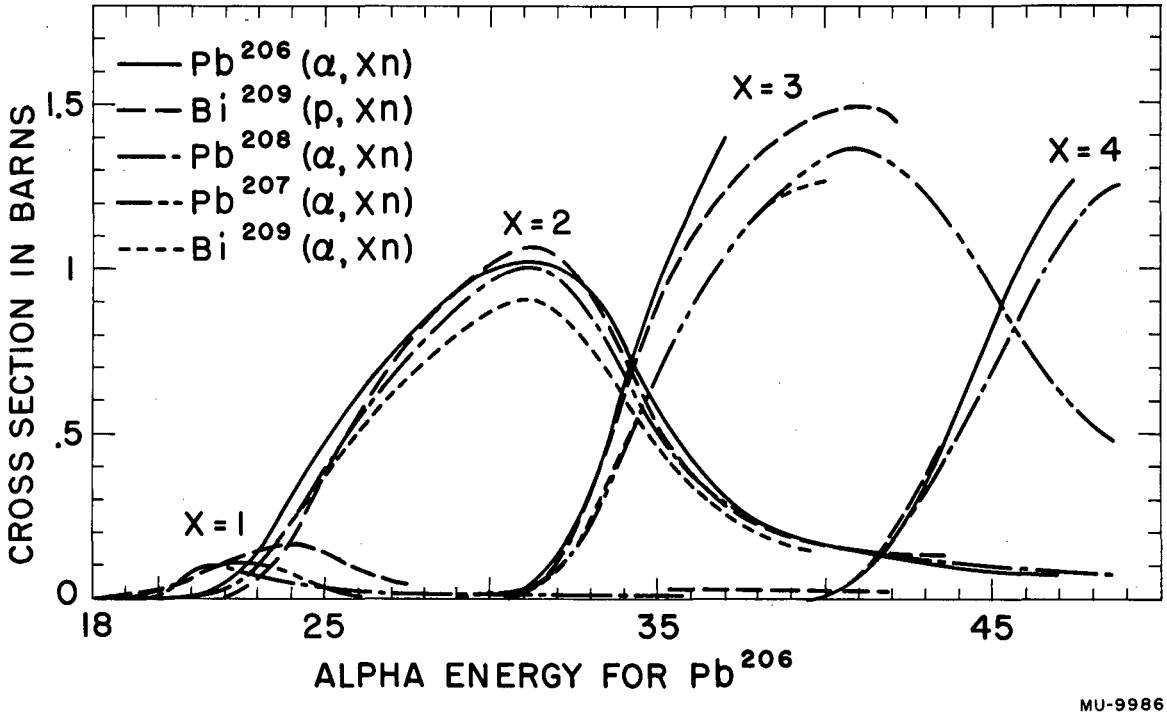

Fig. 9. Comparison of the excitation functions for lead and bismuth. The curves for lead are based on the data of this experiment. The $Pb^{208}(\alpha, n)$ data is taken from Ref. 20, the bismuth data from Refs. 6 and 7. The energy scale applies to reactions on Pb^{206}. For the energy scales of the other curves see Table VIII.

in the tables of Stern[30] and Glass, Thompson, and Seaborg[31] are listed in Table VIII.

The (a, 2n), (a, 3n) and (a, 4n) reactions are remarkably similar for all target nuclei. The (a, n) reactions do not match in shape as well as the others. The reaction $Pb^{208}(\alpha, n)Po^{211}$ is probably not as accurate as the other (a, n) reactions since it was necessary to sum the cross sections for the formation of the two very short-lived Po^{211} isomers. The observed similarity of the excitation functions is in general agreement with the expectations of the statistical theory. We note for example that the evaporation formula (See Sec. I) predicts that the excitation functions for (a, 2n) reactions on neighboring nuclei will be nearly the same if their thresholds are matched.

The energy shifts which were employed to match the curves in Fig. 9 may be compared to the calculated shifts from the differences in thresholds. The reaction $Pb^{207}(\alpha, n)Po^{210}$ was compared to the reaction $Bi^{209}(p, n)Po^{209}$. The relative energy shift observed to match thresholds is $E_p - E_\alpha = -11.9$ Mev. The shift calculated from the difference between the thresholds is -9.7 Mev. The discrepancy is 2.2 Mev. The discussion of errors in Sec. V, 1 also applies in general to this section. The errors for the (a, n) curves are somewhat higher.

The observed energy shift for $Pb^{208}(\alpha, 2n)Po^{210}$ relative to $Pb^{206}(\alpha, 2n)Po^{208}$ is $E_\alpha(Pb^{208}) - E_\alpha(Pb^{206}) = -1.1$ Mev. The calculated shift is -0.1 Mev. The correction from laboratory to center-of-mass coordinates is negligible here. The observed shift was verified in the enriched Pb^{206} bombardment where both reactions were present, giving a check independent of the beam energy determination. The discrepancy is outside of the errors.

The observed energy shift for $Bi^{209}(\alpha, 2n)At^{211}$ relative to $Pb^{206}(\alpha, 2n)Po^{208}$ is $E_\alpha(Bi^{209}) - E_\alpha(Pb^{206}) = -0.8$ Mev. The calculated shift is $+0.6$ Mev. The discrepancy is 1.4 Mev. The observed energy shift for $Bi^{209}(\alpha, 3n)At^{210}$ relative to $Pb^{207}(\alpha, 3n)Po^{208}$ is $E_\alpha(Bi^{209}) - E_\alpha(Pb^{207}) = 0.0$ Mev. The calculated shift is -1.6 Mev.

Table VIII

Energy shifts for Fig. 9. The bombarding energy was increased by the amount given under "Observed energy shift".

Reaction	Observed energy shift (Mev)	Shift calculated from masses (Mev)
$Pb^{206}(\alpha, xn)Po$	≡0	≡0
$Pb^{207}(\alpha, n)Po^{210}$	0[a]	...
$Pb^{207}(\alpha, 3n)Po^{208}$	1.3	...
$Pb^{208}(\alpha, n)Po^{211}$	0.2[a]	...
$Pb^{208}(\alpha, 2n)Po^{210}$	1.1	0.1
$Pb^{208}(\alpha, 4n)Po^{208}$	1.7	...
$Bi^{209}(p, xn)Po$	11.9[b]	10.4
$Bi^{209}(\alpha, 2n)At^{211}$	0.8	-0.6
$Bi^{209}(\alpha, 3n)At^{210}$	1.3	...

[a] Matched to $Bi^{209}(p, n)Po^{209}$. See Sec. V, 2 for discussion.

[b] See Sec. V, 1 for discussion including correction to center-of-mass coordinates.

Thus the observed energy shifts do not agree with the shifts calculated from the differences in thresholds. The observed shift in the case of $Pb^{208}(\alpha, 2n)Po^{210}$ compared to $Pb^{206}(\alpha, 2n)Po^{208}$ is the most accurately determined. The measured excitation functions are being compared well above their thresholds. The cross sections are not as reliable near the threshold because of interference between reactions and straggling effects. The reason for the discrepancies between observed and calculated energy shifts is perhaps more complicated here than in the preceeding section since the compound nuclei formed in the reactions are not the same. Statistical theory in its simplest form does not explain the discrepancy as may be seen from the evaporation formulae. We will not attempt to explain the discrepancy here.

From the comparison of the reactions $Pb^{208}(\alpha, 4n)Po^{208}$ and $Pb^{206}(\alpha, 4n)Po^{206}$, the Po^{206} mass is calculated to be 206.0446 ± ~0.002 amu. From the comparison of the reactions $Pb^{207}(\alpha, 3n)Po^{208}$ and $Pb^{206}(\alpha, 3n)Po^{207}$, the Po^{207} mass is calculated to be 207.0452 ± ~0.002 amu. These masses are calculated on the Stern scale. On the Glass, Thompson, and Seaborg scale they would be 206.0443 and 207.0449. The errors are estimated from the discrepancies between the observed and calculated energy shifts for the reactions involving known masses.

Deuteron-induced reactions should be considered separately. Kelly[6] and Kelly and Segrè[7] have measured the excitation functions for the reactions (d, n), (d, p), (d, 2n), and (d, 3n) on Bi. When the deuteron-induced reactions are compared to the alpha- and proton-induced reactions on Bi, qualitative differences are seen. The differences are most pronounced for the (d, n) and (d, p) reactions. This is probably because of the importance of stripping processes.[34] The (d, 2n) excitation function is more similar to the (α, 2n) and (p, 2n) excitation functions, indicating that compound nucleus formation is probably more important.

The similarities of the observed excitation functions for alpha- and proton-induced reactions indicate that the excitation

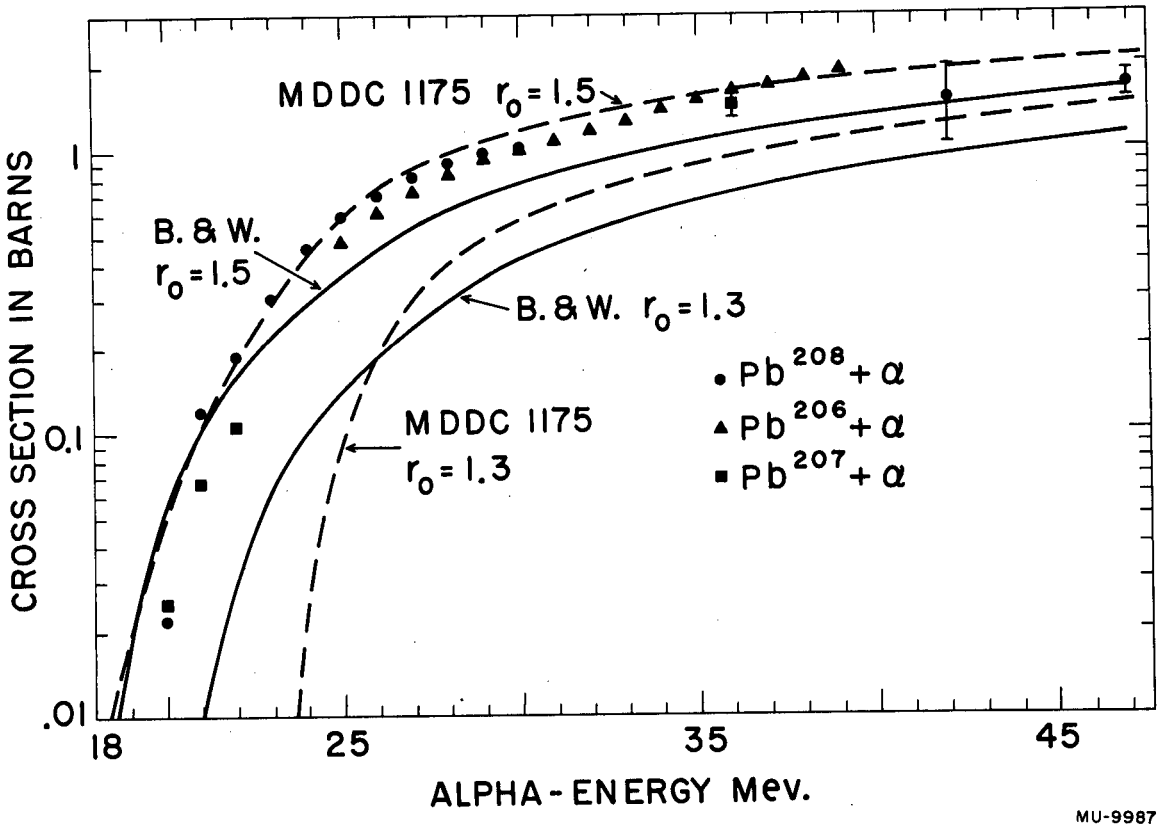

Fig. 10. Total cross sections for alphas on lead. Experimental points are shown. Theoretical values are shown in dotted lines (Ref. 2) and solid lines (Ref. 3).

functions for other isotopes in the region may be estimated from them. However, the excitation functions may be displaced in energy by one or two Mev from that calculated from the thresholds.

3. Total Cross Sections

In Fig. 10 total cross sections have been plotted as a function of energy. The points with uncertainties shown depend on the half life for Po^{209}. The points are calculated for $T_{1/2}$ = 100 years; the uncertainties show the effect of ± 50 years on the calculations. For comparison the theoretical total cross sections calculated by Weisskopf in MDDC-1175[2] and by Blatt and Weisskopf[3] are shown. Values for lead were obtained by graphical interpolation. The experimental points fit the MDDC-1175 calculations with $r_o = 1.5 \cdot 10^{-13}$ cm. In the region of highest accuracy of the cross sections, ~27 to 33 Mev, the value $r_o = 1.48 \cdot 10^{-13}$ cm is obtained. The Blatt and Weisskopf values for $r_o = 1.5 \cdot 10^{-13}$ cm are about 25% lower than the experimental points. This is well outside the experimental errors. The radius of interaction used by Blatt and Weisskopf is $R = r_o A^{1/3} + \rho$, $\rho = 1.2 \cdot 10^{-13}$ cm. The radius used in the MDDC-1175 calculations is not stated, but appears to have been nearly the same since the quoted barriers are nearly the same.

ACKNOWLEDGMENTS

The author is grateful to Professor Emilio Segrè for suggesting this experiment and supporting its execution. The author thanks Dr. Elmer Kelly for instructive discussion concerning his bismuth experiments.

Mr. Albert Ghiorso lent the use of the alpha pulse-height analyzer. Mr. Dan O'Connell of the Accelerator Technicians, University of California Radiation Laboratory, carried out the enriched-lead isotope evaporations. The enriched Pb^{206} and Pb^{207} were supplied by the Oak Ridge National Laboratory, the Pb^{208} by the nuclear chemistry group of the Radiation Laboratory. The high-purity natural lead and its spectroscopic analysis were supplied by Mr. George M. Gordon, U. C. Division of Mineral Technology. Dr. Hans Bichsel and Dr. R. F. Mozley kindly supplied their range-energy data for protons in aluminum. Dr. Ann Birge lent the use of some target apparatus. The 60-inch cyclotron staff gave efficient cooperation for the bombardments. Mr. George Merkel assisted with the bombardments.

This work was supported by the U. S. Atomic Energy Commission.

REFERENCES

1. N. Bohr, Nature 137, 344 (1936).
2. V. F. Weisskopf, Lecture Series in Nuclear Physics, MDDC-1175, U. S. Govt. Printing Office, 1947.
3. J. M. Blatt and V. F. Weisskopf, Theoretical Nuclear Physics (John Wiley and Sons, Inc., New York, 1952).
4. S. N. Ghoshal, Phys. Rev. 80, 939 (1950).
5. P. Morrison, Experimental Nuclear Physics, Vol. II, E. Segrè, editor (John Wiley and Sons, Inc., New York, 1953).
6. E. L. Kelly, "Excitation Functions of Bismuth", (Thesis) University of California Radiation Laboratory Report No. UCRL-1044, Dec. 1950.
7. E. L. Kelly and E. Segrè, Phys. Rev. 75, 999 (1949).
8. H. L. Bradt and D. J. Tendham, Phys. Rev. 72, 1117 (1947).
9. J. P. Blaser, F. Boehm, P. Marmier, and D. C. Peaslee, Helv. Phys. Acta 24, 3 (1951).
10. B. L. Cohen, Phys. Rev. 81, 184 (1951).
11. J. W. Meadows, Phys. Rev. 91, 885 (1953).
12. P. C. Gugelot, Phys. Rev. 93, 425 (1954).
13. Brookhaven Conference on Statistical Aspects of the Nucleus, BNL-331 (C-21) (1955).
14. O. Hirzel and H. Wäffler, Helv. Phys. Acta 20, 373 (1947).
15. E. B. Paul and R. L. Clarke, Can. J. Phys. 31, 267 (1953).
16. B. L. Cohen, E. Newman, R. A. Charpie, and T. H. Handley, Phys. Rev. 94, 620 (1954).
17. R. M. Eisberg and G. Igo, Phys. Rev. 93, 1039 (1954).
18. R. A. Glass, "Studies in the Nuclear Chemistry of Plutonium, Americium, and Curium and the Masses of the Heaviest Elements". (Thesis) University of California Radiation Laboratory Report No. UCRL-2560, April 1954.
19. D. H. Templeton, J. J. Howland, and I. Perlman, Phys. Rev. 72, 758 and 766 (1947).
20. F. N. Spiess, Phys. Rev. 94, 1292 (1954).
21. H. Bischsel and R. F. Mozley, private communication.

22. H. Bichsel and R. F. Mozley, Phys. Rev. 94, 764 (1954) (A).
23. J. H. Smith, Phys. Rev. 71, 32 (1947).
24. W. A. Aron, B. G. Hoffman, and F. C. Williams, AECU-663 (Second Revision 1949).
25. E. L. Kelly, Phys. Rev. 75, 1006 (1949).
26. H. Bethe and J. Ashkin, Experimental Nuclear Physics, E. Segrè, editor, Vol. I, p. 244 (John Wiley and Sons, Inc., New York, 1953).
27. B. B. Rossi and H. H. Staub, National Nuclear Energy Series, Manhattan Project Technical Section Div V, Vol 2, Ionization Chambers and Counters (McGraw-Hill Book Co., Inc., New York, 1949).
28. A. Ghiorso, A. H. Jaffey, H. P. Robinson, and B. B. Weissbourd, "A 48-Channel Pulse-Height Analyzer for Alpha-Energy Measurements", paper 16.8, National Nuclear Energy Series, Manhattan Project Technical Section Div IV, Vol 14B, The Transuranium Elements, G. T. Seaborg, J. J. Katz, and W. M. Manning, editors (McGraw-Hill Book Co., Inc., New York, 1949).
29. E. L. Kelly, private communication.
30. M. O. Stern, Revs. Modern Phys. 21, 316 (1949).
31. R. A. Glass, S. G. Thompson, and G. T. Seaborg, J. of Inorganic and Nuclear Chemistry, Vol 1, No. 1, 3, (1955).
32. K. T. Bainbridge, Experimental Nuclear Physics Vol. 1, E. Segrè, editor, (John Wiley and Sons, Inc. New York, 1953).
33. H. Feshbach, C. E. Porter, and V. F. Weisskopf, Phys. Rev. 96, 448 (1954).
34. D. C. Peaslee, Phys. Rev. 74, 1001 (1948).
35. J. M. Hollander, I. Perlman, and G. T. Seaborg, Revs. Modern Phys. 25, 469 (1953).